Supporting Information

Achieving highly efficient CO_2 to CO electroreduction exceeding 300 mA/cm^2 with single atom nickel electrocatalysts.

Hui-Yun Jeong [a], Mani Balamurugan [a], Venkata Surya Kumar Choutipalli [d,e], Eun-suk Jeong [f], Venkatesan Subramanian [d,e], Uk Sim*[c], Ki Tae Nam*[a,b]

a. Department of Materials Science and Engineering, Seoul National University Seoul 08826, Republic of Korea. E-mail: nkitae@snu.ac.kr
b. Research Institute of Advanced Materials, Seoul 08826, Republic of Korea
c. Department of Materials Science and Engineering, Chonnam National University, Gwangju 61186, Republic of Korea. E-mail: usim@jnu.ac.kr
d. Inorganic and Physical Chemistry Laboratory, CSIR-Central Leather Research Institute, Adyar, Chennai-600 020, India
e. Academy of Scientific and Innovative Research (AcSIR),CSIR-CLRI Campus, Chennai-600 020, India.
f. Department of Physics Education and Institute of Fusion Science, Jeonbuk(Chonbuk) National University, Jeonju 54896, Republic of Korea.

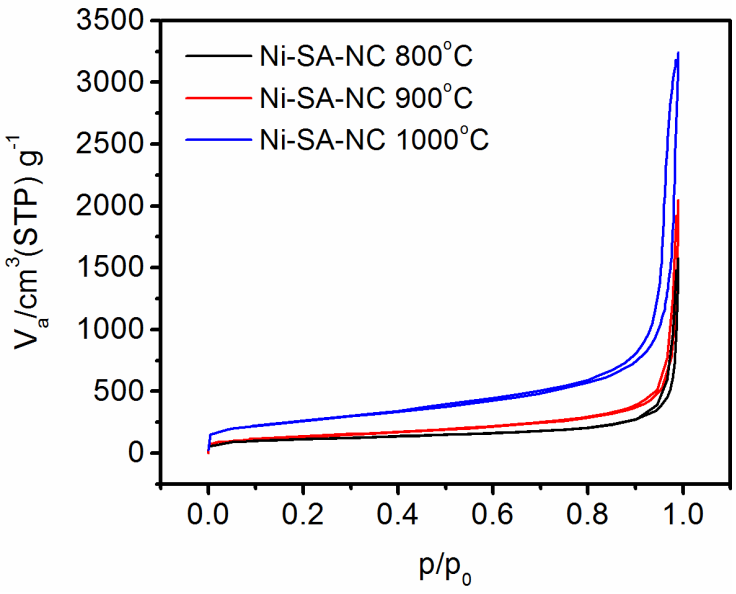

Figure S1. Nitrogen adsorption-desorption isotherms of nickel and nitrogen doped three dimensional porous carbons (Ni-SA-NCs).

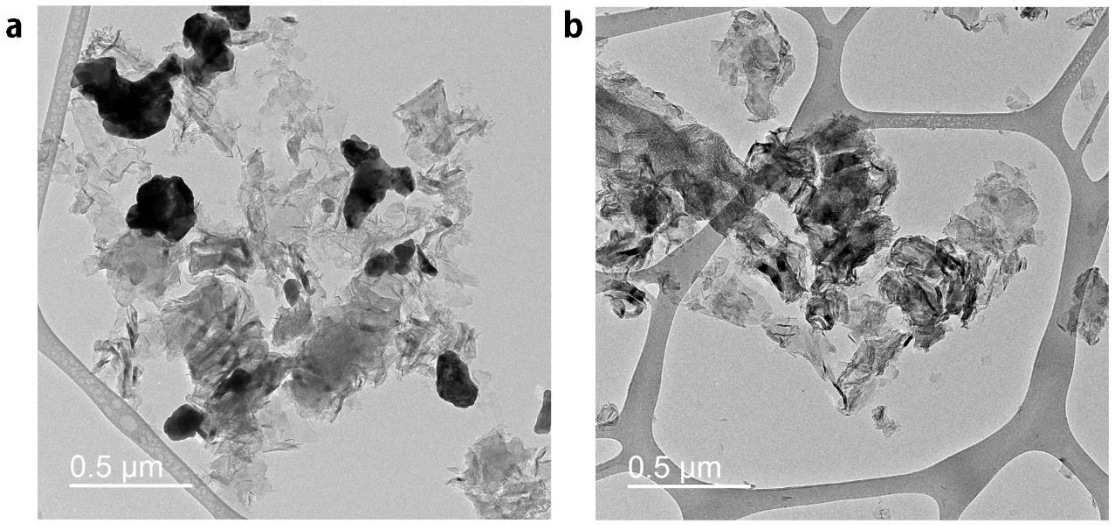

Figure S2. TEM images of carbonization products of nickel chloride dissolved EMIM-DCA without silica templates. (a) Before acid etching, nickel agglomerates can be observed. (b) After acid etching, most of the nickel agglomerates are efficiently removed.

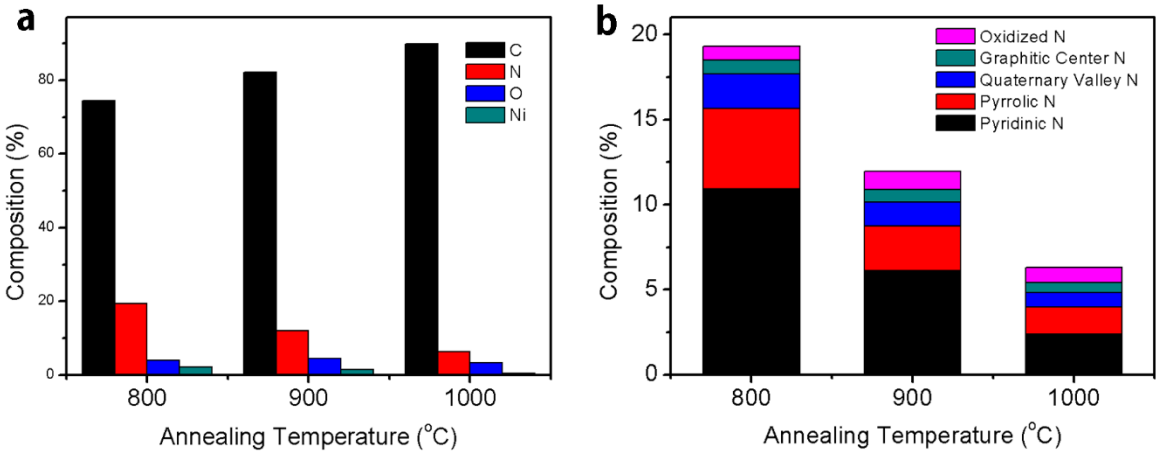

Figure S3. Atomic composition of single atom nickel and nitrogen doped three dimensional porous carbon (Ni-SA-NC). (a) Atomic composition of Ni-SA-NCs (b) Composition of each nitrogen species.

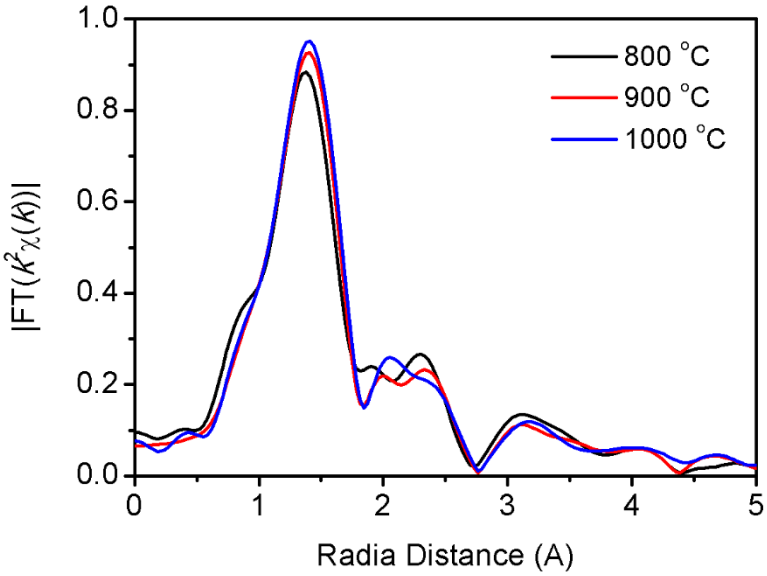

Figure S4. Extended X-Ray Absorption Fine Structure (EXAFS) spectra of Ni-SA-NCs. The increase in the peak intensity is observed as the carbonization temperature increases, and, indicates the change in the coordination number around nickel atoms.

Table S1. EXAFS fitting results of Ni-N-RGO based on the single metal atom substituted divacancy model, S_O^2, amplitude reduction factor determined from Ni foil fitting as a reference; CN, coordination number; R, distance between absorber and backscattering atoms; σ^2, Debye-Waller factor; ΔE_0, inner potential correction; R, R-factor;

Ni-SA-NC	Paths	S_O^2	CN	R (Å)	σ^2 (Å ^{2})	ΔE_0 (eV)	R, %
1000 °C	Ni-N	0.79	3.9	1.864	0.006	1.8	0.1
900 °C			3.8	1.864	0.006	1.5	0.1
800 °C			3.6	1.864	0.006	-3.3	0.6

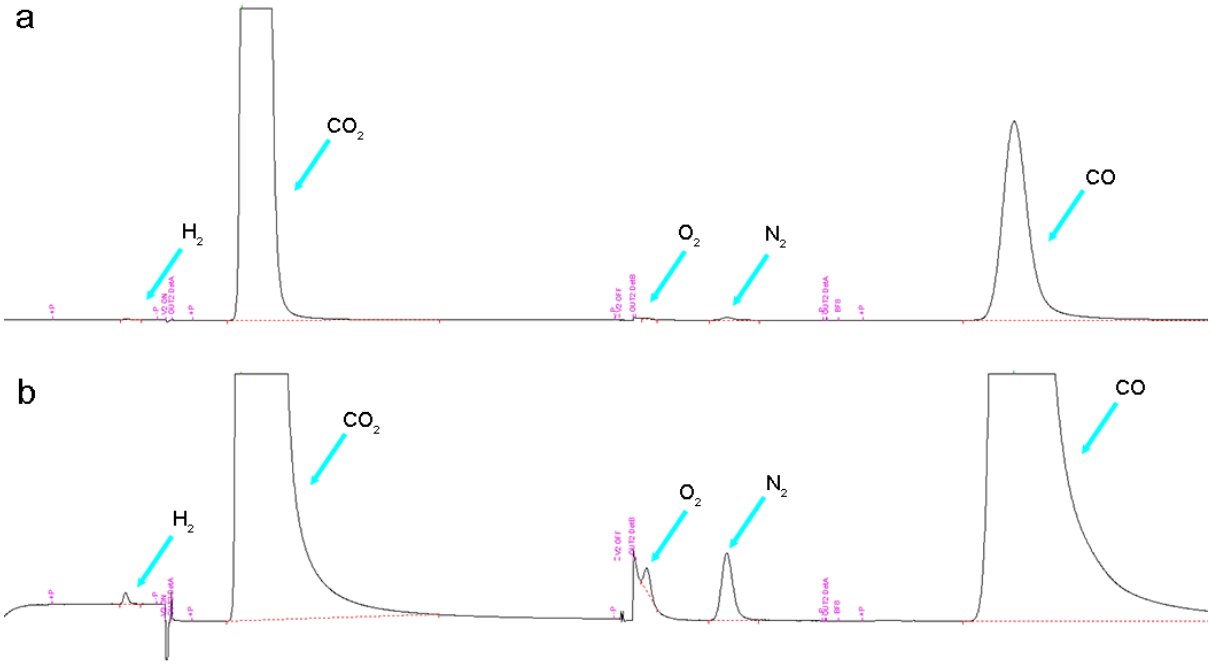

Figure S5. Gas chromatography spectrum of the head space gases after bulk electrolysis (0.5 M $KHCO_3$, -1.0 V vs. RHE, 2000 s). (a) CO is detected as a major CO2 reduction products. (b) magnified GC spectrum, only small amount of hydrogen is detected and small amount of air (oxygen and nitrogen) was permeated during the gas sampling.

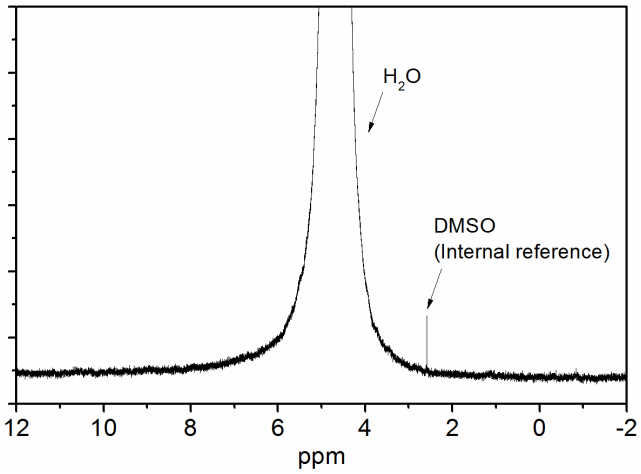

Figure S6. ^1H NMR spectrum of the electrolyte after bulk electrolysis (0.5 M $KHCO_3$, -1.0 V vs. RHE, 2000 s), DMSO was added as an internal reference. And, no noticeable liquid products were detected

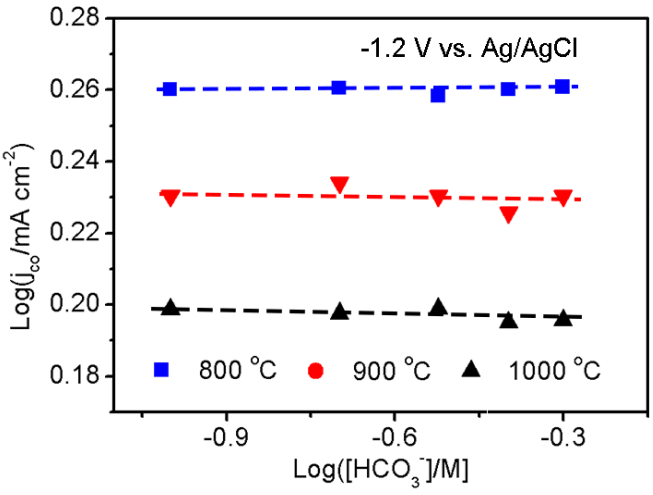

Figure S7. The CO partial current density plotted against the bicarbonate ion concentration. Corresponding slope is close to 0, suggesting that the CO_2 reduction reaction is independent on the bicarbonate ion concentrations.

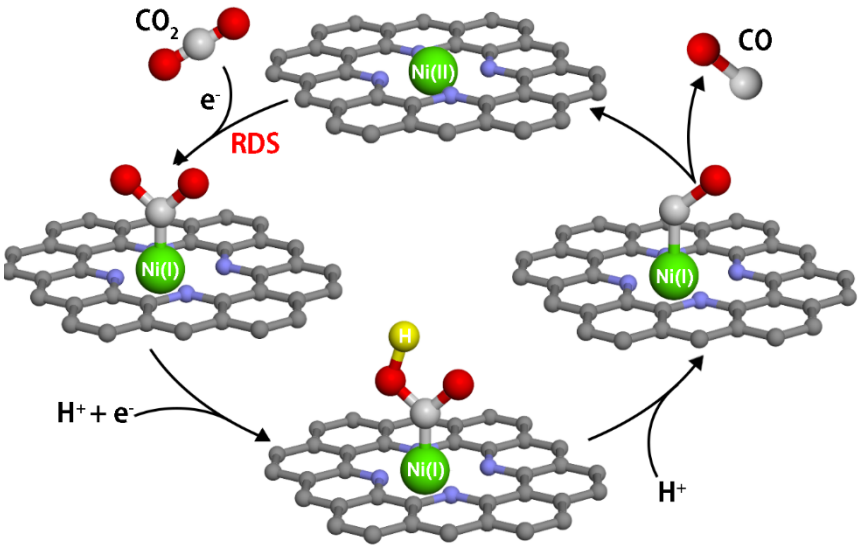

Figure S8. Proposed CO_2 reduction reaction mechanism for single atom nickel on the Ni-SA-NCs

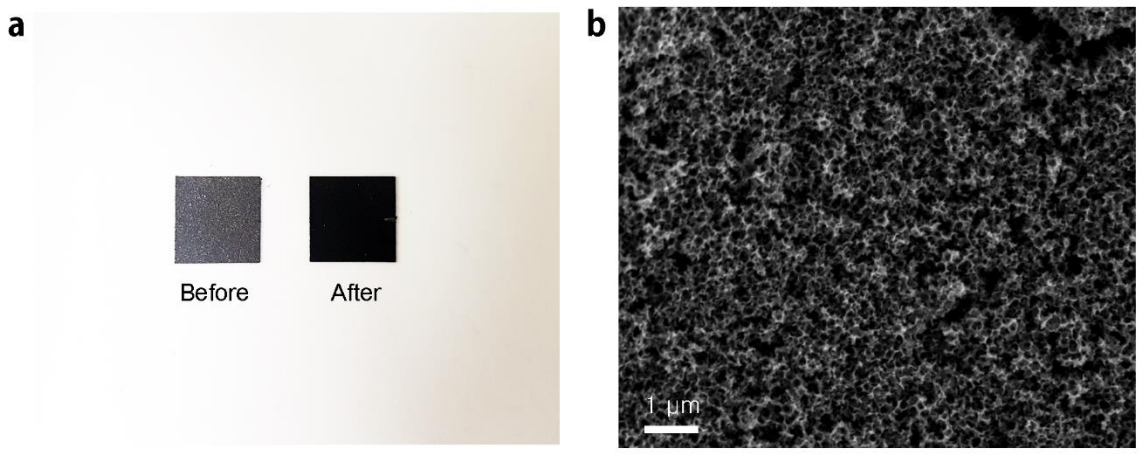

Figure S9. Photography of gas diffusion layer (GDL, AvCarb GDS1120) before and after Ni-SA-NCs deposition. Surface morphology of Ni-SA-NCs coated GDL.

Table S2 Comparisons of Ni-NG catalyst with reported nickel based CO_2 to CO electroreduction catalysts

Catalyst	CO FE (%)	J (mA/cm2)	Potential (V)	Reference
Ni-SA-NC	**98**	**380**	**3.0 V (MEA)**	**This work**
Ni-SA-NC	**98**	**145**	**2.6 V (MEA)**	**This work**
Ni-SA-NC	**99**	**26**	**-0.8 V vs RHE (0.5M KHCO3)**	**This work**
Ni-NG	97	51.5	2.78 V (MEA)	*Energy Environ. Sci*., 2018,**11**, 893-903
Ni-NG	95	11	-0.73 V vs RHE (0.5M KHCO3)	*Energy Environ. Sci*., 2018,**11**, 893-903
C-Zn1Ni4 ZIF-8	98	22	-0.83 V vs RHE	*Energy Environ. Sci*., 2018,**11**, 1204-1210
A-Ni-NG	98	22	-0.72 V vs RHE (0.5M KHCO3)	*Nature Energy* 2018, **3**, 140–147
Ni-N-C	93	3.9	-0.67 V vs RHE 0.5 M KHCO3	*ACS Catal.* 2018, **8**, 6255−6264
Ni-N4-C	99	28	−0.81 V vs RHE (0.5M KHCO3)	*J. Am. Chem. Soc.* 2017, **139**, 14889−14892
Ni-N-C	85	12	-0.78V vs RHE (0.1M KHC)3)	*Nat. Commun.* 2017, **8**, 944
Ni SAs/N-C	72	6.5	-0.9 V vs RHE (0.5M KHCO3)	*J. Am. Chem. Soc.* 2017, **139**, 8078−8081
Ni-N-Gr	75	0.2	-0.65 V vs RHE (0.1M KHCO3)	*Small* 2016, **12**, 6083–6089